

Ionic thermal current of concentrated cubic solid solutions of $\text{SrF}_2\text{:LaF}_3$ and $\text{BaF}_2\text{:LaF}_3$

H. W. den Hartog and J. C. Langevoort

Solid State Physics Laboratory, 1 Melkweg, 9718 EP Groningen, The Netherlands

(Received 10 February 1981)

In this paper we present new results of ionic-thermal-current (ITC) experiments on concentrated solutions of SrF_2 and BaF_2 on one hand and LaF_3 on the other. The concentration range of the trivalent La impurities is 0–20 mol %. In earlier work we have shown that even for moderate La concentrations there are significant effects of defect-defect interactions on the ITC results for dipole reorientation. The present work is concerned with polarization effects in doped alkaline-earth fluorides, which are not associated with dipolar complexes but with space charges. In contrast with the results for dipoles, where the ITC peak is located at a fixed temperature as a function of the concentration of the dipoles, we find that the depolarization peak associated with space charges shifts towards lower temperatures with increasing La concentrations. In order to explain this observation we have investigated a new relaxation process, which is in fact a combination of two processes. It appears that with this model we can understand the important features of the experimental results obtained in this investigation.

I. INTRODUCTION

In general one observes three ionic-thermal-current (ITC) bands in alkaline-earth fluoride crystals containing small amounts of trivalent impurity ions. There are two peaks which are located at temperatures well below room temperature; these bands are ascribed to dipole reorientation. The dipoles associated with these bands are usually called nearest-neighbor (NN) and next-nearest-neighbor (NNN) dipoles; a three-dimensional schematic representation of NN and NNN dipoles has been given in Fig. 1.

The dipole complexes have been studied by means of various different experimental techniques such as EPR, electron-nuclear double resonance (ENDOR), ITC, and optical spectroscopy.^{1–8} The interaction between the dipoles has been investigated in our laboratory using the different techniques and the observations may lead to consistent conclusions for the strength of the interactions as a function of the impurity concentration, etc.^{9,10}

The third ITC peak, which is usually located at about room temperature, has not been studied in great detail up to now, although this peak has some remarkable and interesting properties: Its intensity is large as compared to that of the dipole peaks at low temperatures and the peak position varies signi-

ficantly as the concentration of trivalent impurity ions is changed. The latter feature especially is in contrast with the observations made for dipole reorientation, where we have shown that the position of the ITC band does not depend upon the concentration of the defects; the width of the band increases with increasing concentrations.^{9,11}

Another feature of the high-temperature (HT) band has been observed by Laredo *et al.*¹²; the intensity of this band is influenced very drastically by mechanical treatment of the sample. From this observation these authors conclude that the HT band

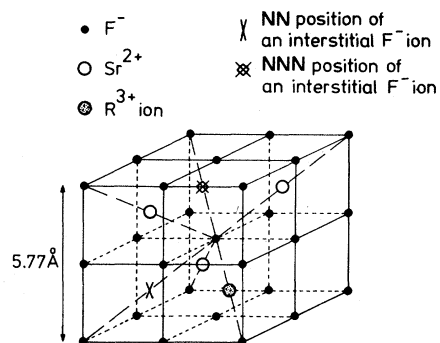


FIG. 1. Three-dimensional schematic representation of an SrF_2 crystal showing the structure of a tetragonal (type I) and a trigonal (type II) $R^{3+}\text{-F}_i^-$ complex.

should be connected with phenomena associated with dislocation lines. On the other hand, Laredo *et al.* did not observe any shift of the ITC band as a result of the mechanical treatment. It should be noted that due to mechanical deformations, dislocations will move through the samples. The mobility of defects and impurities in alkaline-earth fluorides is small as compared to that of the dislocation lines. In untreated samples in the neighborhood of dislocations there is an accumulation of defects and impurities, which after the deformation will be separated from the dislocation lines to some extent, leading to an increase of some of the ITC bands.

It is the purpose of this paper to report about the features of the HT band in BaF_2 doped with appreciable concentrations of LaF_3 (up to about 20 mol %). The results of the ITC measurements will be interpreted in terms of a combination of two different jump mechanisms: (a) a mechanism that consists of a free jumping interstitial fluoride ion, and (b) a jumping F^- interstitial neighboring a lanthanum impurity. It will be shown that this charge-transport mechanism leads to an ITC peak with a variable peak position.

At low concentrations the HT band is determined predominantly by jumping free interstitials, which can be deduced from the measured jump activation energy. At high La concentrations the HT band approximately coincides with the NNN dipole peak, indicating that the jumps associated with this depolarization peak are similar to NNN jumps. It will be proposed that the space charges observed in strongly doped materials are generated by a percolation-type mechanism as described by Kirkpatrick.¹³ The samples can be considered as systems consisting of conducting spheres embedded in isolating hosts. The spheres each contain one dipole; the radius of the spheres is assumed to be equal to the dipole length of the NNN $\text{La}^{3+}-\text{F}_i^-$ complex. The ITC results can be explained reasonably well with this model.

II. EXPERIMENTAL PROCEDURES

The doped materials were prepared with a high-frequency crystal-growing machine; the raw materials, i.e., mixtures of SrF_2 and LaF_3 or BaF_2 and LaF_3 were placed in carbon crucibles with inner diameters of 8 mm together with approximately 2 mol % PbF_2 which is used to remove the O^{2-} impurities. The mixed crystals are grown at a rate between 3 and 6 mm/h under a purified He atmosphere of about 600 mm Hg.

At low La concentrations (< 5 mol %) the crystals are cleaved easily along {111} planes; for concentrations larger than 5 mol % we employed a slide wire saw to cut the samples for the ITC experiments. The cryostat and the setup in which the samples are mounted are described by Lenting *et al.*¹⁴ The heating rate is controlled by a heating coil powered by a proportional integrating differentiating (PID)-type temperature controller. The set point of the controller is kept constant, while the thermocouple electromotive force (emf) is compensated by a linearly varying voltage. The ITC experiments in this setup are carried out between 77 and 350 K, which limits our possibilities to study one of the depolarization effects (the HT peak) for the system $\text{SrF}_2:\text{La}^{3+}$ in the low-concentration range because here this band is located at temperatures higher than 350 K. The polarization voltage used for these experiments is 4000 V, the average thickness of the samples is 1.5–2.0 mm and the heating rate is 0.04–0.05 K/sec.

The concentration of the La impurities for the various $\text{BaF}_2:\text{La}^{3+}$ samples has been measured with the x-ray fluorescence method. We found that this method can be used for concentrations higher than 1 mol %, because the peaks associated with Ba and La are very close to each other and for La concentrations the La peak is obscured by the presence of the very intense Ba peak. The intensities of the x-ray fluorescence spectra of the crystals used for our ITC experiments were compared with intensities found for carefully mixed powders with known concentrations of BaF_2 and LaF_3 . For reliable x-ray results it is necessary to crush the ITC samples; in that way the geometry of the calibration and the determination of the concentrations in the unknown sample is found to be equal.

III. EXPERIMENTAL RESULTS

We have shown in earlier papers that the reorientation behavior associated with dipoles is influenced significantly if the concentration of these dipoles increase above a value⁹ of approximately 10^{18} cm^{-3} . For concentrations higher than 10^{19} cm^{-3} the defect structure may be affected: This has been observed by Aalbers and den Hartog¹⁰ for the system $\text{SrF}_2:\text{Gd}^{3+}$ where the ratio of NN and NNN concentration varies by more than a factor of 6.

At low La concentration in SrF_2 we only observe the so-called NN peak, which is located about 150 K (see also van Weperen and den Hartog¹¹). Increasing the La concentration we find a new peak developing at about 210 K, which is assigned to

NNN dipoles. The HT peak is situated at temperatures well above 300 K. A survey of the results for $\text{SrF}_2:\text{La}$ has been given in Fig. 2. For concentrations of 2.5 mol % and higher the HT peak is located below 300 K and moves to lower temperatures with increasing La concentrations. It can be seen from Fig. 2 that the NN and the NNN peaks are situated at fixed positions.

Similar observations have been made for the system $\text{BaF}_2:\text{La}$; in Fig. 3 it is shown that at low concentrations both the NN and the NNN peak are present and the HT peak is situated at approximately 300 K. Here too, the strength of the NNN peak relative to that of the NN peak increases with increasing La concentration. The HT peak shifts towards low temperatures until it reaches a position which approximately coincides with that of

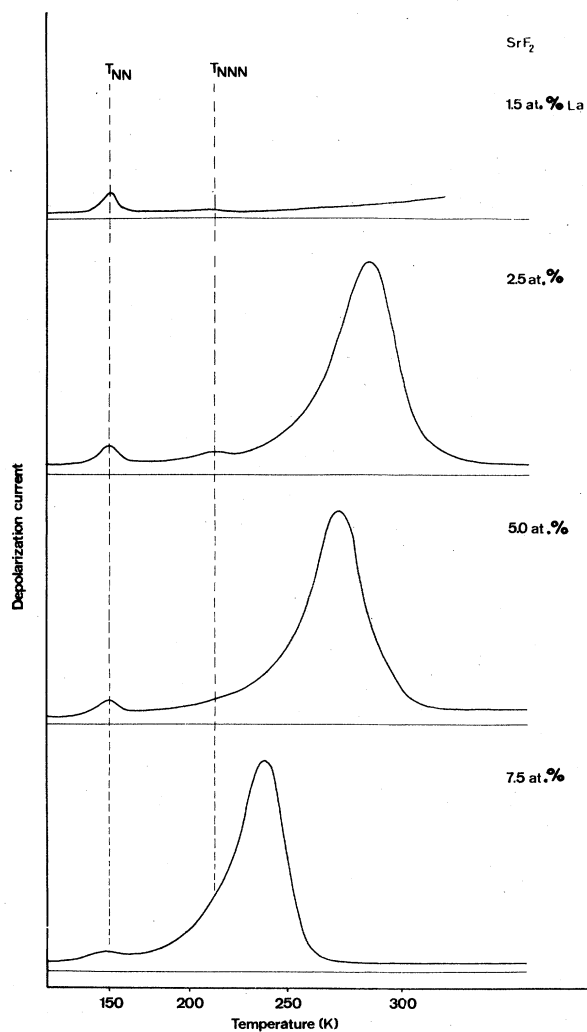


FIG. 2. Survey of the ITC results for $\text{SrF}_2:\text{La}$ crystals in the concentration range 0–7.5 mol % LaF_3 .

the NNN peak; in this region the shifts of the HT peak are small.

For the system $\text{BaF}_2:\text{La}$ we have determined the concentrations of the La impurities in the samples used for the ITC experiments. With x-ray fluorescence we were able to determine La concentrations ≥ 1 mol %. The results of the measurements on $\text{BaF}_2:\text{La}^{3+}$ have been compiled in Table I together with the nominal La concentrations; we note that we have used the ITC samples to determine the concentration and therefore the results can be related directly with the ITC results.

In Fig. 4 we have given the plot of the position of the HT peak versus the measured La concentration. It shows that at lower concentrations the peak shifts very rapidly. Unfortunately, we were not able to

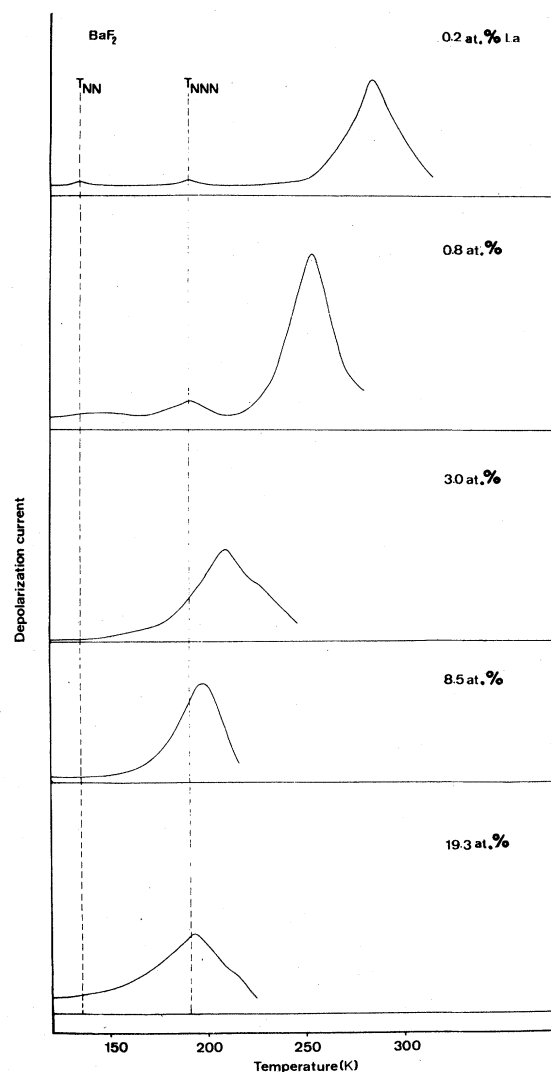


FIG. 3. Survey of the ITC results for $\text{BaF}_2:\text{La}$ crystals in the concentration range 0–20 mol % LaF_3 .

TABLE I. HT-peak positions and La concentrations of the BaF₂:La samples investigated.

Sample no.	T_{\max} (K)	Concentration (mol %)	
		nominal	measured
1	253	0.8	1.4
2	237	3.1	1.8
3	223	1.9	2.3
4	209	3.0	3.8
5	206	6.0	4.7
6	206	8.0	5.1
7	200	6.5	5.5
8	196	9.0	6.3
9	198	8.5	7.8
10	194	19.3	11.2
11	191	25.9	13.5
12	194	44.8	19.3

investigate this region in detail as a result of the limitations of the x-ray fluorescence method. For concentrations higher than about 8 mol % the HT-peak position is approximately constant, and it is located at about the position of the NNN dipole peak as can be seen from Fig. 3.

IV. THEORY

As mentioned before, the high-temperature peak behaves in a different way as compared to the NN and NNN dipole peaks. With increasing concentration the peak moves towards lower temperatures, whereas a dipole peak is located at an approximately fixed position. This implies that the behavior of the HT band cannot be explained simply by a broadening of the ITC activation energy about a fixed average value E_0 described by the formula

$$N(E) = \frac{N_d}{pV\pi} \exp\left[-\frac{(E - E_0)^2}{p^2}\right], \quad (1)$$

where p is the broadening parameter and N_d is the total number of dipoles of the type considered. We assume that the characteristic relaxation time τ_0 in the formula

$$\tau = \tau_0 \exp\left[\frac{E}{kT}\right]. \quad (2)$$

has a fixed value. The results of the broadening of the distribution of activation energies is a broadening of the ITC peak; especially the high-temperature tail of the reorientation band deviates significantly from the unperturbed ITC band (see Fig. 5). The position of the band, however, remains unchanged.

Therefore, in order to explain the gradual shift of

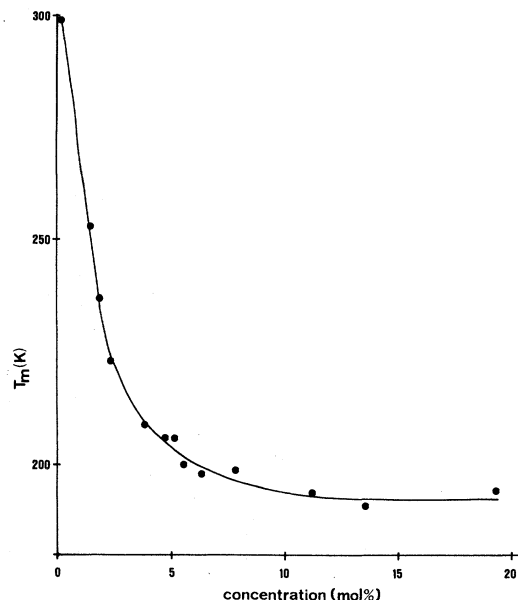


FIG. 4. Behavior of the HT reorientation peak as a function of the La concentration in BaF₂.

the band as a function of the La concentration, we have to propose an alternative model. We assume that the HT band is due to the formation of space charges opposite to the electrodes. These space charges consist of interstitial fluoride ions (in the neighborhood of the anode) and the La³⁺ impurities (opposite to the cathode). Only the interstitial fluoride ions are mobile and, consequently, we focus our attention on these defects. It turns out that in pure alkaline-earth fluorides there are interstitial fluoride ions which move through the crystal with an activation energy¹⁵ of 0.7–0.9 eV, depending on the host crystal under consideration. This thermally activated jump process together with the polarizing electric field gives rise to the polarization charges at the electrodes. During depolarization the reverse process takes place. When trivalent impurities are added local charge compensation centers of the types shown in Fig. 1 are formed. Part of the trivalent ions, however, will be situated at cubic positions and will act as traps for interstitial F⁻ ions, which move through the crystal.

If an interstitial F⁻ is trapped by a trivalent impurity ion, this interstitial ion will make dipole jumps, which have activation energies ranging from 0.4–0.6 eV (see Refs. 11 and 14). On the other hand, existing dipoles may dissociate, giving rise to free interstitials. Thus, the polarization process producing the HT band is governed by two types of jumps (jumps of free interstitials and reorienting and dissociating dipoles) simultaneously. From this we

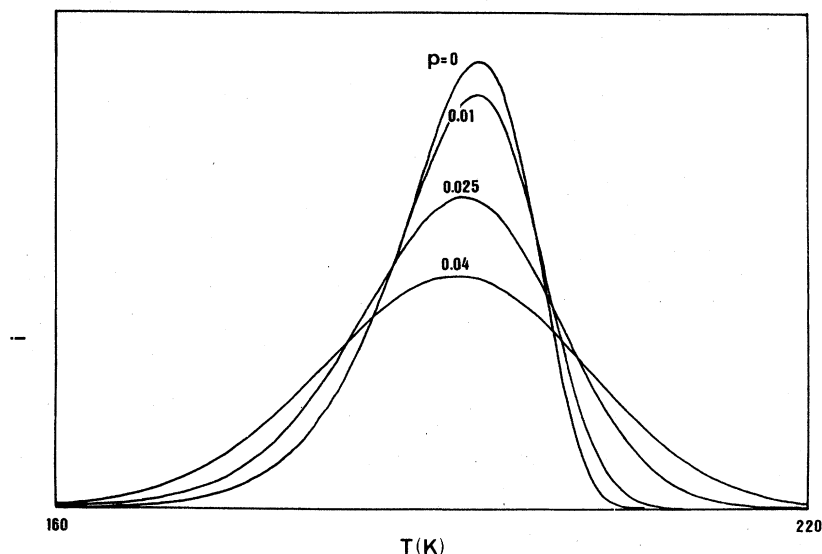


FIG. 5. Calculated ITC curves for different broadening parameters (p). Note that, because we are dealing with dipole reorientation, the ITC band position is approximately constant.

calculate the following expression for the relaxation time:

$$\frac{1}{\tau} = \frac{(1-\alpha)}{\tau_{\text{free interstitials}}} + \frac{\alpha}{\tau_{\text{dipoles}}}, \quad (3)$$

where α is the probability of a free interstitial fluoride ion to make a dipolelike jump. For simplicity we define α as follows. Consider an F^- ion placed at an interstitial position in the crystal doped with La^{3+} ions. Some of these impurity ions are not compensated by nearby interstitial F^- ions. α is the probability of placing the interstitial in the neighborhood of a free La^{3+} impurity such that either a dipole of the NN type or an NNN dipole is formed. It follows that in the low-concentration

limit α depends upon the concentration of La^{3+} ions and the dissociation constant of the dipoles.

In accordance with the combined relaxation process, outlined above, we calculate for the depolarization current as measured with the ITC method

$$I(T) = \frac{dP}{dt} = B \exp \left[- \int_0^T \frac{dT'}{b\tau(T')} \right] / \tau(T), \quad (4)$$

where b is the heating rate and B is a proportionality constant. For calculations we have taken the characteristic relaxation times associated with the dipole and those of the free interstitials to be equal to 2.3×10^{-14} and 2×10^{-12} sec, respectively. The corresponding activation energies have been chosen to be $E_d = 0.6$ and $E_f = 0.8$ eV. In Fig. 6 we

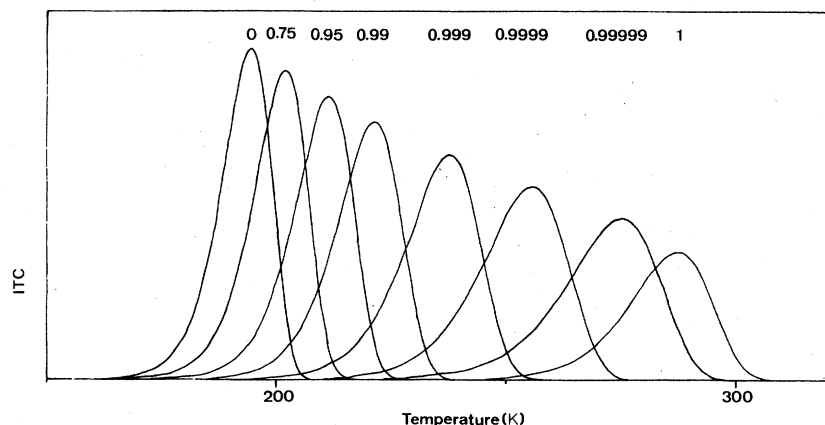


FIG. 6. Calculated depolarization peaks based on the mechanism described by Eqs. (3) and (4). Note that the band moves towards low temperatures with decreasing values of α . For each of the peaks the value of $(1-\alpha)$ has been indicated.

have plotted the theoretical ITC curves based on the relaxation behavior as described in (3) and it can be seen that the position of the reorientation peak varies as a function of α . For $\alpha = 1$ the peak is located at the NNN dipole position; for $\alpha = 0$, on the other hand, the peak is determined by the properties of the jumping free interstitial F^- ions. At the interval $0 \leq \alpha \leq 10^{-2}$ the position of the ITC band varies very rapidly and this variation should clearly be compared with the large variations of T_{\max} observed experimentally (Fig. 4) for low La concentrations. It is concluded that there is qualitative agreement between the model described above and experiment. A more detailed analysis of the theoretical and experimental T_{\max} versus concentration curves provides us with information about the charge-transport processes in these materials.

At low temperature the conduction process can be described by means of jumping free F^- interstitials, which are perturbed by the presence of the trivalent impurities. When the La concentration is increased, however, it is hard to maintain this approximation because the individual dipoles interact rather strongly and the interstitial F^- ion trapped by one particular La impurity may switch to another La ion. In an ideally statistical solid solution this leads to a percolation-type conduction mechanism, which has been treated by Kirkpatrick.¹³ We know, however, that in our samples with large amounts of La there is appreciable clustering, which results in a higher critical percolation concentration (x_c).

Kirkpatrick¹³ describes the charge transport by means of a schematical three-dimensional network of lattice points, which may or may not be connected by a resistance. From this model this author obtains—for a simple cubic array of lattice points—a critical concentration of connections (with a resistance) of 30%. Below this concentration there is no charge transport; above this value the transport increases in accordance with the relation

$$T = A(x - x_c)^s, \quad (5)$$

where s has a value between 1.5 and 1.6; A is a constant. Formula (5) appears to be in reasonable agreement with the experimentally observed relationship by Lightsey,¹⁶ who has found that s is about 1.8. It should be noted that the concentration occurring in (5) is a volume ratio; the sample is assumed to consist of two materials: (a) an isolating material and (b) a conducting material. In order to apply this very crude model to our samples we assume that the isolating material is the host crystal

containing free interstitials and the conducting material is a solid consisting of dipole systems, which jump very rapidly as compared to the free F^- interstitials. It is obvious that the volume associated with one NNN dipole is much larger than the volume of one XF_2 molecule in the host crystal; in fact it is about 11 times as large. This means that, in order to calculate the volume ratio, we have to multiply the concentration of NNN dipoles by 11. If this assumption is correct the critical concentration of NNN dipoles should be between 2% and 3%.

If we assume for a moment that the charge transport is determined predominantly by the dipole-type jumps, the conductivity should be proportional to α [which occurs in Eq. (3)]. In Fig. 7 we have plotted α as a function of the La concentration. The values for α have been obtained by comparing the experimental positions of the HT bands with the theoretical results shown in Fig. 6. The behavior of α can be understood in terms of the percolation model for charge transport. Above a certain La concentration α increases very rapidly. We have fitted the α values to a behavior

$$\alpha = B(x - x_c)^s, \quad (6)$$

where we have chosen for s a value of 1.8 (in accordance with the value reported by Lightsey¹⁶). The best fit is obtained for $x_c = 2.2$ mol %, which corresponds, if the above-mentioned volume correction factor is applied, with a percentage of 24. We note that this value is close to the value calculated by Kirkpatrick,¹³ especially when we realize that the model is a rather crude one.

Apart from the very rapid changes of T_{\max} versus

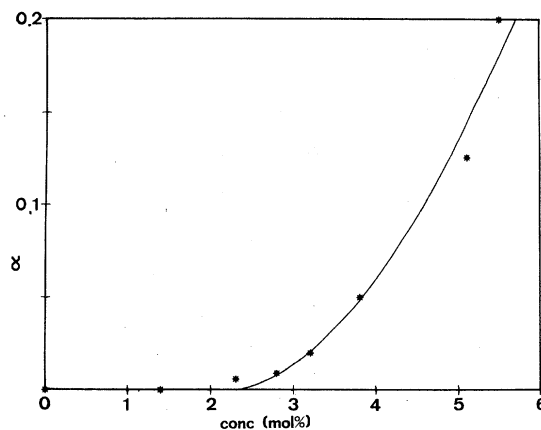


FIG. 7. Plot of the value of α as a function of the La concentration in BaF_2 . The values of α have been calculated from the positions of the ITC peaks observed experimentally.

the concentration in the low-concentration region ($c < 2$ mol %) we observe in Fig. 3 that in the high-concentration region the HT bands shifts only rather slowly. It should be noted that until now we have assumed that the characteristic parameters E and τ_0 for the various jump processes do not change as a function of the R^{3+} concentration. This is probably approximately true for the low-concentration region but at high concentrations E and τ_0 may change gradually as a result of, for instance, the changes of the lattice constant of these solid solutions. This trend for the HT peak is probably also present in the low-concentration region, but it cannot be observed of the rapid variations due to the mechanism described above.

Until now we have—for the combined transport mechanism—not taken into account the effect of defect-defect interactions, which were shown to be important for the dipole reorientation kinetics and ionic conductivity. We have to assume that the relaxation times $\tau_{\text{free interstitials}}$ and τ_{dipoles} are characterized by two different distributions of activation energies centered at E_f and E_d , respectively; the widths of the two distribution functions are expected to be different. We estimate that the width of the activation energy distribution associated with free interstitials is larger than that of the dipoles because the interaction between a monopole and neighboring charged or dipolar defects is stronger than the corresponding interaction for a central dipole. In situations where the jump process is determined by dipole jumps or free interstitial jumps alone, the broadening of the distribution of activation energies leads to a broadening of the corresponding ITC bands. If both jumps contribute to the transport process the broadening of the activation energies will produce a broadened ITC band; in addition, slight changes in the position of the ITC band are expected because of the difference of the broadening parameters associated with E_f and E_d . These latter effects have not been investigated in detail.

From the above discussion we derive the following conclusions about the conductivity properties of heavily doped fluorite materials. Neglecting the slight variations of the activation energies due to small changes of the lattice parameter as a function of the R^{3+} concentration, we find that in the extrinsic conductivity region the ionic conductivity—taking into account the broadening of the activation energy—is

$$\sigma = \sigma_0 \exp \left[- \left(\frac{E_f}{kT} - \frac{p^2}{4k^2T^2} \right) \right] \quad (7)$$

If the concentration is increased, the effective activation energy decreases due to defect-defect interaction. For concentration between 1 and 3 mol % we have found that “dipole jumps” contribute significantly to the charge transport; therefore the conductivity cannot be described anymore by Eq. (7) and, consequently, an extra term should be added to account for the new transport process. At concentrations larger than 6 mol % the transport process is determined predominantly by the above-mentioned dipole-dipole jumps. This results in a conductivity

$$\sigma = \sigma'_0 \exp \left[- \left(\frac{E_d}{kT} - \frac{(p')^2}{4k^2T^2} \right) \right] \quad (8)$$

As mentioned above, the activation energy E_d is lower than E_f and the broadening parameter p' for dipoles is smaller than the corresponding parameter p for free interstitials. In an ionic conductivity measurement one will find an effective activation energy (at high concentrations) of

$$E^* = E_d - \frac{(p')^2}{4kT} \quad (9)$$

From (9) we see that E^* is temperature dependent; in the temperature region of interest (600–1200 K) this dependence is only weak even if we choose rather large values for p' . Taking for $E_d = 0.60$ eV and for $p' = 0.2$ eV, E^* varies between 0.40 and 0.50 eV in this temperature range. An interesting feature of the model proposed here is that the ionic conductivity is described by an activation energy which is approximately one-half of the normal value E_f .

The above-described lowering of the activation energy can be quite significant at low temperatures (300–400 K). Even if the basic mechanism consists of jumps with an ordinary activation energy of 0.6 eV the broadening effects may bring the effective activation energy down to values between 0.1 and 0.2 eV. In this regard it is of interest to note that superionic (and nonstoichiometric) Na β -alumina has an activation energy of about 0.1 eV, whereas for stoichiometric material an activation energy of 0.6 eV has been observed.¹⁷ We know that in normal nonstoichiometric Na β -alumina the defect concentration is quite high (probably about 20 at. %). It is possible that the drastic decrease of the activation energy is due to strong defect-defect interactions; if this is the case the broadening parameter is approximately 0.25 eV.

Until now no detailed studies on defect-defect interactions exist. The discussion given above suggests that, in order to understand the transport phenomena in high defect materials, it is necessary that de-

tailed knowledge about the various interactions between the defects is available. There are interactions of different nature; one can distinguish between electrostatic, polarization, and elastic interactions. New methods should be developed which allow us to investigate the various types of interaction between defects. It is clear that our experimental results until now only provide us with information about the total strength of the interactions between

the defects.

A systematic investigation on the defect-defect interactions can be carried out if detailed information about the defect structure exists. Especially in heavily doped materials one should be aware of clustering, but also defect-defect interactions may affect the concentration ratios of the various defects quite significantly.

-
- ¹E. L. Kitts, Jr. and J. H. Crawford, Jr., *Phys. Rev. B* **9**, 5264 (1974).
²A. D. Franklin and S. Marzullo, *J. Phys. C* **3**, L171 (1970).
³P. D. Southgate, *J. Phys. Chem. Solids* **17**, 1623 (1966).
⁴D. R. Tallant, D. S. More, and J. C. Wright, *J. Chem. Phys.* **67**, 2897 (1977).
⁵P. P. Yaney, D. M. Schaeffer, and J. L. Wolf, *Phys. Rev. B* **11**, 2460 (1975).
⁶J. M. Baker, E. R. Davies, and T. Rs. Reddy, *Contemp. Phys.* **13**, 45 (1972).
⁷M. J. Weber and R. W. Bierig, *Phys. Rev.* **134**, A1492 (1964).
⁸A. Edgar and H. K. Welsh, *J. Phys. C* **8**, L336 (1975).
⁹W. van Weperen, B. P. M. Lenting, E. J. Bijvank, and H. W. den Hartog, *Phys. Rev. B* **16**, 2953 (1977).
¹⁰A. B. Aalbers and H. W. den Hartog, *Phys. Rev. B* **19**, 2163 (1979).
¹¹W. van Weperen and H. W. den Hartog, *Phys. Rev. B* **18**, 2857 (1978).
¹²E. Laredo, M. Puma, and D. R. Figueroa, *Phys. Rev. B* **19**, 2224 (1979).
¹³S. Kirkpatrick, *Rev. Mod. Phys.* **45**, 574 (1973).
B.P.M. Lenting, J.A.J. Numan, E. J. Bijvank, and H. W. den Hartog, *Phys. Rev. B* **14**, 1811 (1976).
¹⁵W. Bollmann, P. Görlich, W. Hauk, and H. Mothes, *Phys. Status Solidi A* **2**, 157 (1970).
¹⁶P. A. Lightsey, Ph.D. thesis, Cornell University, 1972 (unpublished).
¹⁷W. Hayes, *Recent Developments in Condensed Matter Physics* (Plenum, New York, in press).